Sensor and Simulation Notes

Note 402

25 October 1996

Design Guidelines for Flat-Plate Conical Guided-Wave EMP Simulators With Distributed Terminators

D.V. Giri

Pro-Tech, 47 Lafayette Circle, #364, Lafayette, CA 94549-4321

and

Carl E. Baum

Phillips Laboratory, Kirtland AFB, NM 87117

Abstract

In this note, we describe the electromagnetic design considerations of a flat-plate conical guided-wave simulator with distributed terminators. Such a simulator permits the propagation of a spherical, transverse electromagnetic (TEM) mode between the two conductors. This class of nuclear electromagnetic pulse (NEMP) simulators can be energized either by a high-voltage transient pulse or a low-level continuous wave (CW) source.

Contents

Acknowledgment

We are thankful to Dr. D. McLemore of Kaman Sciences Corporation, Mr. Bill Prather and Mr. Tyron Tran of Phillips Laboratory for their guidance and support.

1. *Introduction.*

The electromagnetic objective of a guided-wave simulator is to produce a propagating transient TEM wave, similar to what exists at large distances from an actual EMP generated by a high altitude nuclear explosion [1]. A guided-wave or transmission-line type of EMP simulator is an efficient and convenient system for this purpose.

Historically, the parallel-plate transmission line type of simulator shown schematically in Figure 1, consisted of a pulser, a wave launcher, a central parallel plate region, a wave receptor and a terminator. Examples of such systems are ALECS, ARES, and ATLAS-I in the U.S. In this class of EMP simulators, a transient wave is guided in the air region between the two conductors. Both horizontal (e.g., ATLAS-I) and vertical (e.g., ALECS and ARES) polarization of the electric field are possible in these large, fixed-site installations. A systematic survey of such simulators with over 60 references may be found in [2] and illustrated examples of existing facilities are described in [3]. High field strengths near "threat" level become possible and electromagnetic fields in these transmission line simulators are easily computed for the dominant TEM mode of propagation.

In Figure 1, it is also observed that a conical line is used as wave launcher and a wave receptor on either side of the central parallel-plate region. Impedance and field discontinuities are minimized although never completely eliminated in large structures such as these. Owing to their large sizes, certain engineering compromises to the ideal EM designs become necessary. Yet another characteristic or limitation lies in the fact that such a two-conductor system can support non-TEM modes, if they are excited for any reason. Sources of non-TEM mode excitation can be in the pulser-simulator interface and the two bends where conical lines meet the central cylindrical line.

In order to avoid some of these limitations, an alternative is to build a long conical transmission line and terminate it with a distributed terminator. The advantages of a conical line are:

a) a shorter longitudinal dimension of the simulator for a prescribed working volume;

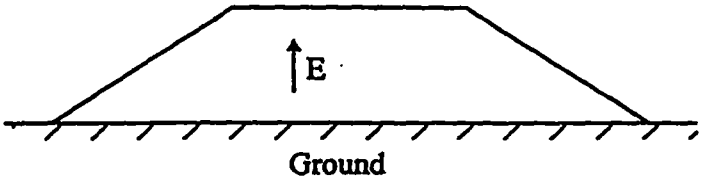

(a) Vertically polarized with flat ground plane

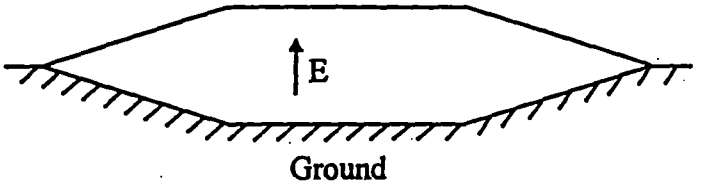

(b) Vertically polarized with ground plane sloped at ends

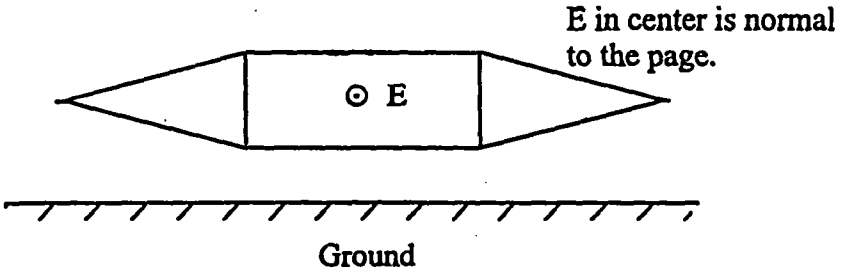

(c) Horizontally polarized and supported above ground

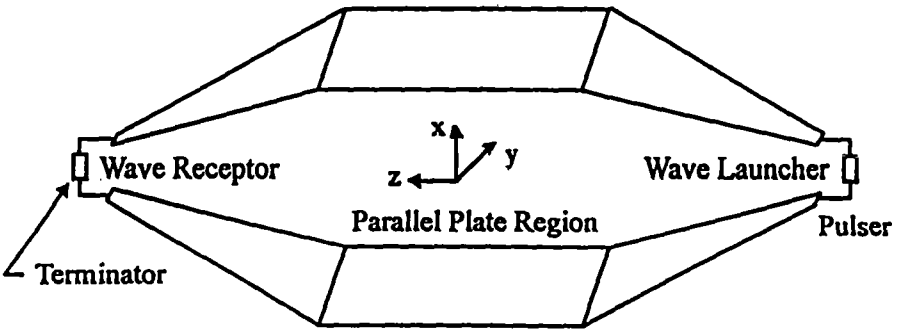

(d) Functional division of this class of simulators

Figure 1. Examples of bounded wave simulators (planar TEM wave in the central region)

b) avoidance of the input and output bend;

c) no termination required for the high frequencies

while the "price" to pay for the above advantages lie in:

- spherical TEM wave approximating a planar TEM wave;
- large distributed termination is inevitable.

An artist's concept of a conical line simulator is shown in Figure 2 and a side view delineating "ideal" and "practical" working volumes is illustrated in Figure 3. The conical-line simulator consists of a pulser, a ground plane, top-plate and a terminator. The top-plate above a ground plane forms one-half of a symmetric conical transmission line. Strictly speaking, such a structure supports and propagates a spherical transient TEM wave and not a planar TEM wave. The implicit assumption here is that the wave front with a large spherical radius approximates a planar wave. The spherical TEM wave is terminated with a characteristic impedance, typically in the range of 80 to 100 Ω, at the end of the line. The "theoretical" (elevated from the ground plane) and "practical" (on the ground plane) working volumes are identified in Figure 3. For some years now, we (the authors) have been helping various European countries with the design of simulators of this type. In the process, we have developed refinements in various aspects of the design. These new simulators represent state of the art for these small-to-medium size conical-transmission-line simulators. Examples include SIEM II in France, DIESES in Germany, VEPES in Switzerland, SAPIENS II in Sweden and INSIEME in Italy. The present paper documents what we have learned in the process.

The analyses of the TEM mode characteristics for such a conical transmission line are well documented [4-6], and are similar to the TEM mode for a flat-plate cylindrical transmission line [7-9] and will not be repeated here. We focus on design guidelines that help in the actual implementation of concepts and in the fabrication of such simulators. Since the distributed terminator is a critical component of this class of NEMP simulators, a lot of attention is given to its design aspects in various sections of this note. This includes considerations such as, a) looking at the terminator as a transmission line, b) an optical view of the terminator, c) matching the current distribution in the top plate to the terminator, d) development of the terminator equivalent circuit , and d) tuning the terminator for optimal performance etc.

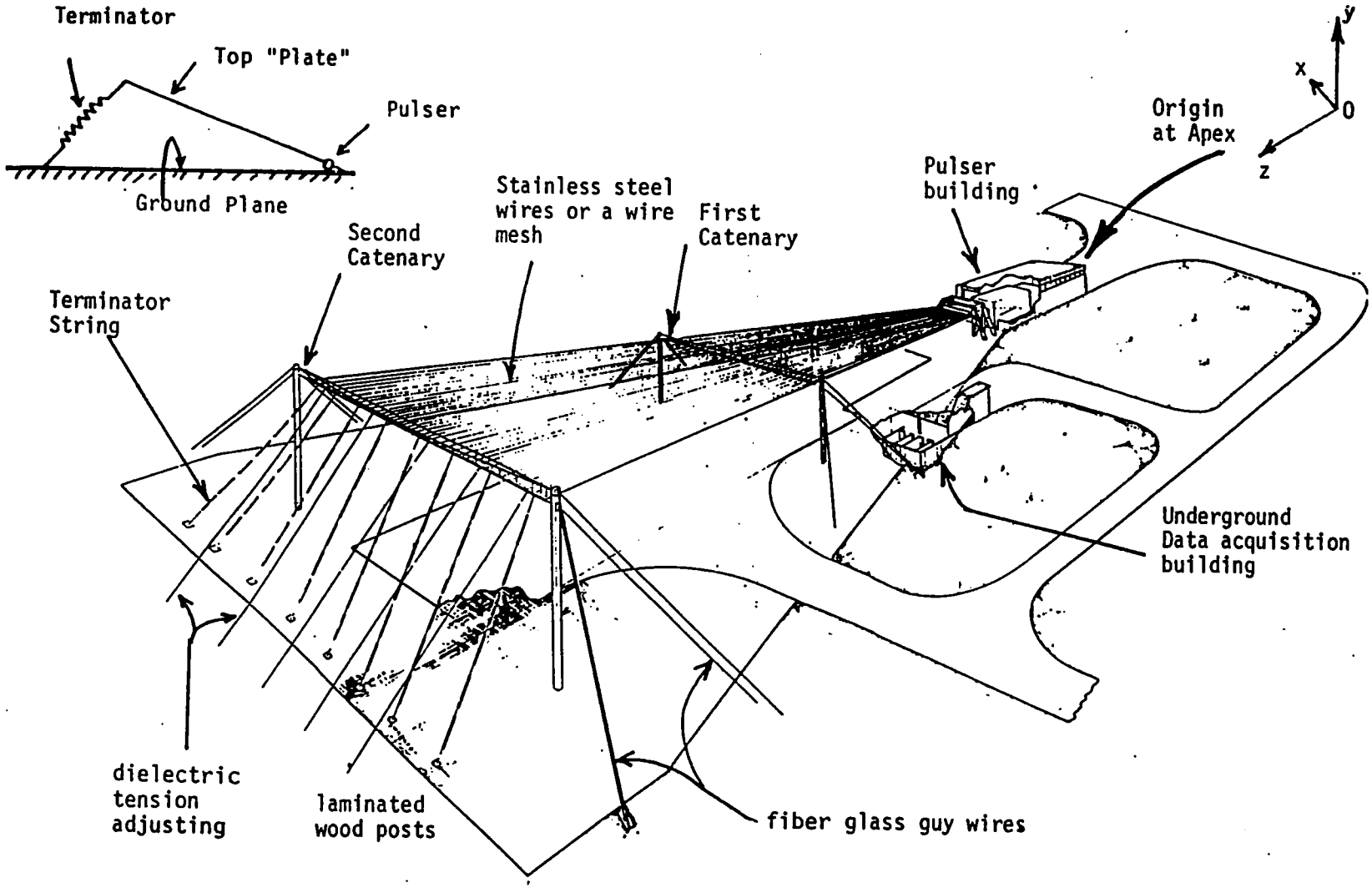

Figure 2. An artist conception of a conical transmission line simulator (spherical TEM wave in the working volume)

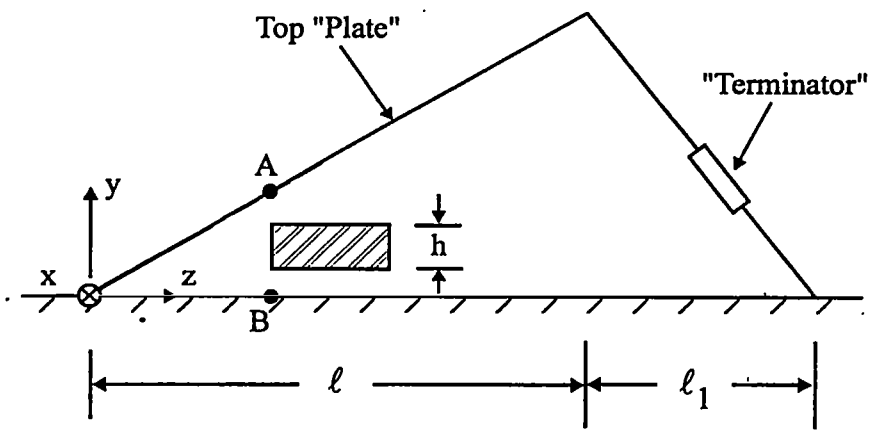

(a) "Theoretical" working volume with AB ≥ 1.6 h when test object can be raised above the ground plane with the use of a dielectric stand.

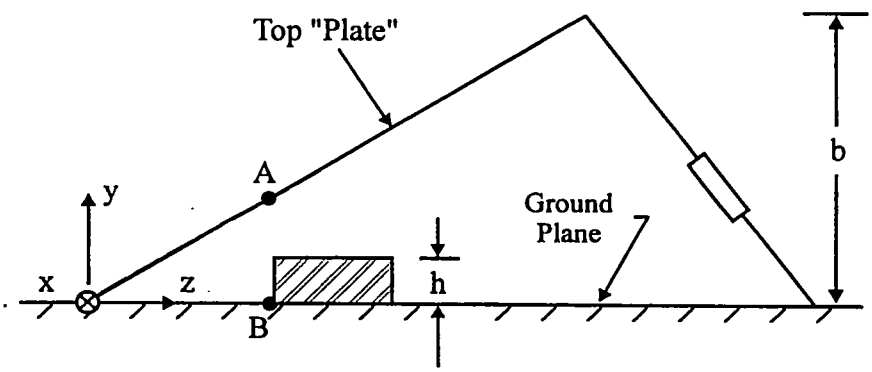

(b) "Practical working volume with AB ≥ 1.6 h when test object cannot be raised above the ground plane, or when the ground plane is used as an image plane

Figure 3. Working volume considerations

2. *Avoiding Higher-Order TEM Modes in Top-Plate and Ground Plane*

The top-plate, if it were a solid plate of metal, would represent one conductor above a ground plane and thus form a one-line in the terminology of multi-conductor transmission lines [10]. However, it is both impractical and undesirable to have a solid top-plate conductor. Various factors such as the supporting the weight of the metallic sheet in open-environment (sun, wind and rain/snow/ice) make this impractical, given the typical sizes of the top plate (several tens of m). Also, while the top-plate is essential for the launching and propagation of the spherical TEM wave, it can adversely impact an NEMP test of an electronic object/system via simulator/object interaction. Early designs constructed the top-plate by a set of N wires as indicated in Figure 4 [7]. In this figure, we illustrate a portion of the top-plate as it goes across a support catenary. Typically, these wires are stainless steel aircraft cables or copper-cladded steel wires etc. It is immediately recognized that such a (N+1) system of conductors including the ground plane, or an N-line can support N TEM modes [11]. There will be one desired or principal TEM mode and (N-1) undesired or parasitic TEM modes. Note also that these N wires are of different lengths, the wires at the edge of the "plate" being the longest, resulting in differential TEM modes and/or resonances between parallel wires when shorted at ends. When the path difference between any two wires becomes an integral multiple of half-wavelengths, higher order modes can be generated at several harmonic frequencies. Since the objective is to launch, propagate and terminate a single TEM wave, it is essential to avoid these differential TEM modes. The solution lies in the use of a wire mesh for the top-plate, or at least sufficient number of transverse conductors in combination with longitudinal conductors. The mesh size is governed by the following factors:

(a) the perimeter p of an individual mesh should be small compared to the shortest wavelength λ_s of interest (say $p \leq \lambda_s/5$), (Figure 5a);

(b) if the above condition is hard to meet for reasons such as ice loading or shorter risetimes in the pulse, then the mesh can be rectangular in shape with its larger dimension along the propagation direction, assuming ($p \sim \lambda_s$) (Figure 5b).

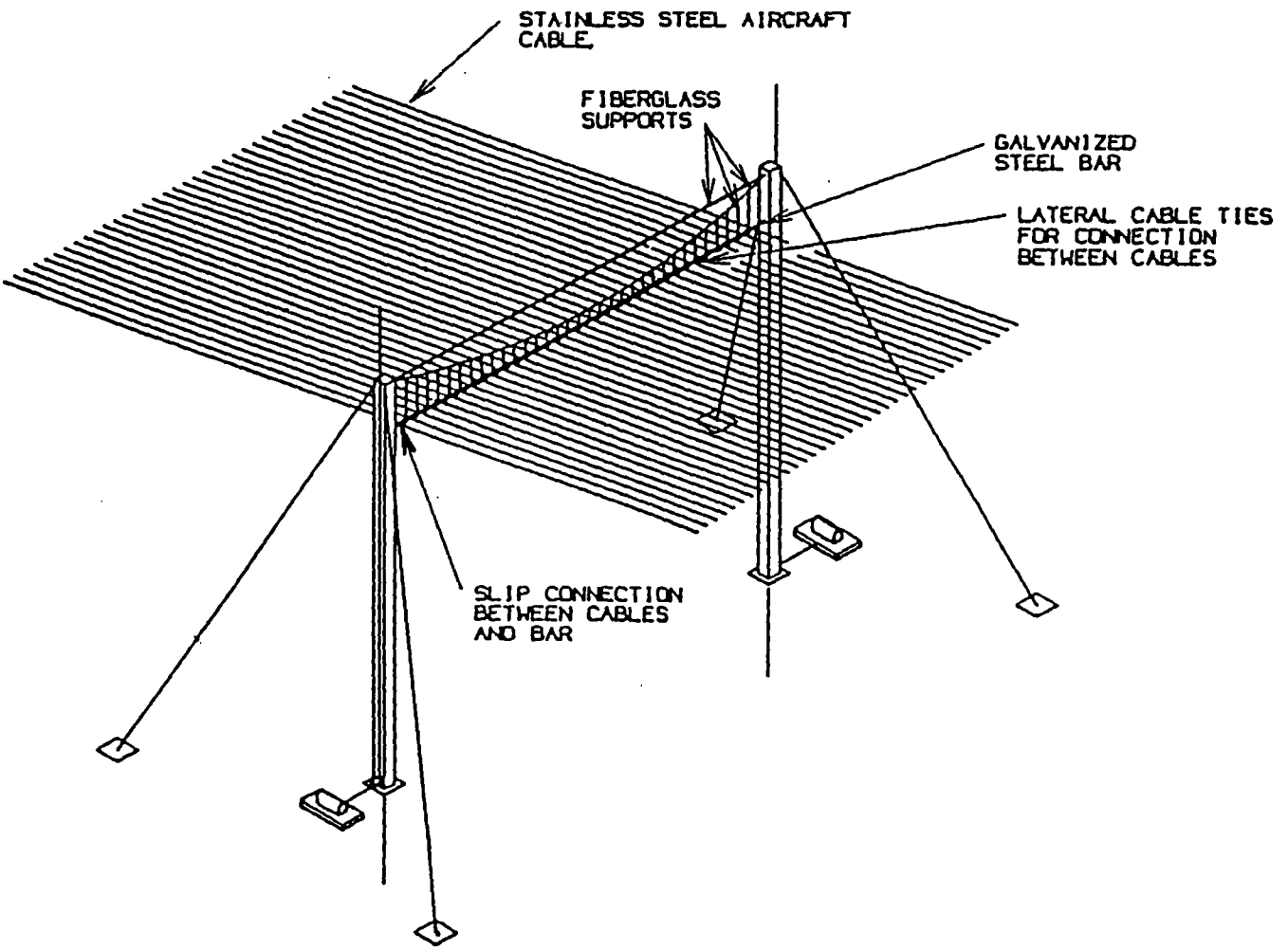

Figure 4. The "top-plate" of the conical transmission line, comprised of N-wires

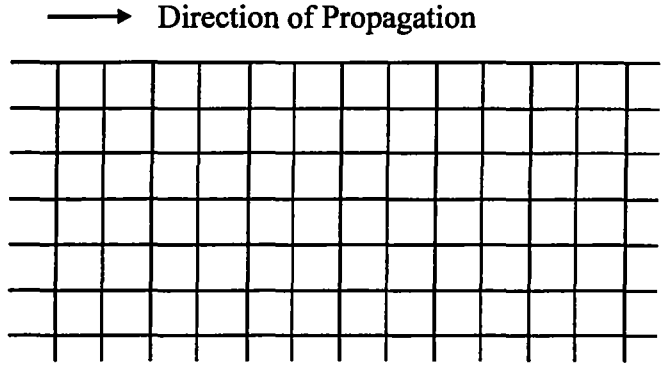

Perimeter $p = 4\,d$

$p \leq \lambda_s/5$

λ_s = shortest wavelength in the pulse

(a) Top-plate made up of square mesh

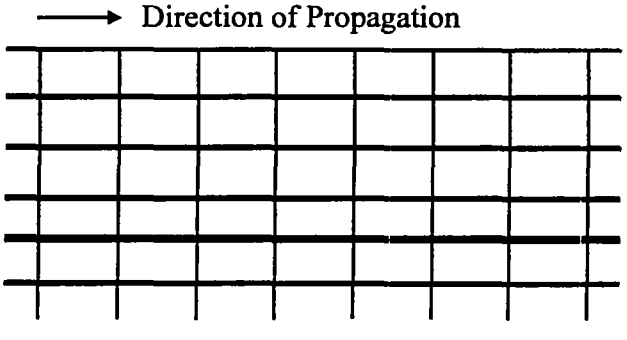

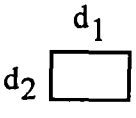

Perimeter $p = 2(d_1 + d_2)$

$p \sim \lambda_s$

(only if (a) is impractical)

(b) Top-plate made up of a rectangular mesh.

Figure 5. Some wire-mesh options for the top-plate

The problem of electromagnetic scattering by square and rectangular meshes has been studied in the past [12], in terms of obtaining the plane wave reflection and transmission coefficients. This formulation is then utilized to treat the surface wave propagation over bonded wire-mesh structures. The numerical results presented in [12] concerning the phase shift as the mesh perimeter p approaches a wavelength, support the design principle that the larger dimension of a rectangular mesh be along the direction of propagation. Next, we can relate the mesh perimeter to the risetime of a double exponential pulse as follows:

$$V(t) = V_0 \left(e^{-\beta t} - e^{-\alpha t}\right) u(t) \quad ; \quad \alpha >> \beta \tag{1}$$

$$\tilde{V}(\omega) = V_o \left[\frac{1}{j\omega + \beta} - \frac{1}{j\omega + \alpha}\right] \tag{2}$$

The upper 3 dB roll-off frequency f_h in the above spectrum can be shown to be

$$f_h \cong \frac{\beta}{2\pi} = \frac{\ell n(9)}{2\pi \left(t_{10-90}\right)} \cong \frac{0.35}{t_{10-90}} \tag{3}$$

corresponding to a shortest significant wavelength λ_s of

$$\lambda_s = \frac{c}{f_h} \cong \left[0.857\ t_{10-90}\ (ns)\right]\ m \tag{4}$$

which leads to the values in Table 1.

Table 1. Bandwidth requirements for a prescribed risetime.

$t_{10\text{-}90}$ (risetime)	f_h	λ_s
10 nsec	35 MHz	8.57 m
5 nsec	70 MHz	4.28 m
2 nsec	175 MHz	1.71 m
1 nsec	350 MHz	0.86 m
500 ps	700 MHz	0.43 m
100 ps	3.5 GHz	0.08 m

It is observed that for a 5 nsec pulse, the 3 dB frequency roll-off occurs at 70 MHz and the mesh perimeter has to be small compared to 4.28 m, which is quite practical. However, as we approach pulse propagation with risetimes of the order of 1 nsec, the mesh perimeter has to be small compared to 86 cm. The ice-loading factor may restrict the mesh perimeter to a number comparable to 86 cm, in which case, a rectangular mesh with the larger dimension along the propagation direction (say 30 cm x 10 cm mesh) is preferable to a square mesh of 20 cm x 20 cm, although both have the same perimeter.

Yet another source of higher-order modes is the simulator/object interaction. As the TEM mode passes by the object, the scattered field from the object could hit the simulator conductors and become re-incident on the object leading to spurious effects. The fields scattered from the test object can launch higher-order TEM modes between wires and propagate energy in both directions (i.e., towards the pulser and towards the terminator). These scattered fields can also launch higher-order TE and TM modes. The higher-order TE and TM modes neither have a planar wave front as in cylindrical transmission lines, (e.g., parallel plate transmission lines), nor a spherical wave front (as in conical transmission lines). This problem is alleviated by restricting the size of the working volume. In each cross-section, if the maximum height of the test object is $\leq$ 60% of the height of the top-plate [9,13,14] the simulator/object interaction problem has been demonstrated to reduce to acceptable levels. This criterion is set from requiring that currents induced on canonical objects (e.g., cylinder) in the simulator does not deviate from its free-space counterpart by more than 20%. One can of course accept a larger deviation (error) if one wishes, but this should be quantified.

In concluding this section, we observe that the top-plate mesh size and the working volume size are chosen according to the design principles outlined above in controlling or avoiding the launching of higher-order TEM or non-TEM modes of propagation in the simulator.

3. *Some Aspects of Ground Plane Design*

The wire mesh considerations discussed in the previous section for the top-plate also apply to the ground plane with one significant difference. While it is impractical to use a solid plate for the top-plate, it is quite practical to use a solid plate in critical portions of the ground plane. The TEM analysis assumes an infinite ground plane while in practice, it is necessarily finite in dimensions. The finite width of the ground plane affects the TEM characteristic impedance [15] as illustrated in Figure 6, in a quantifiable manner. The width of the ground plane exceeds the width of the top-plate 2a by 2d (see Figure 6) and it is preferable to make $d \geq b$ where b is the height of the top-plate from field uniformity considerations [9]. As an example of field uniformity objective, we illustrate the case of $(2b/2a) = 0.5 \equiv$ plate separation/ plate width, in Figure 7. While Figure 7a shows the contours of constant principal electric field, Figure 7b shows the relative deviation of the electric field at any point in the cross-section with respect to the field at the center. Note that this illustration is for a cylindrical transmission line propagating a planar TEM wave which approximates the spherical TEM wave in a small angle conical line or in sufficiently long lines ($\ell \geq 3b$ and $\ell \geq 3a$). It is also observed that the TEM calculations of Figures 6 and 7 are design goals. In practice such a level of field uniformity (Figure 7b) can be approached in spite of the required engineering compromises, brought about by large sizes of such transmission lines.

It is also important to launch a TEM wave from the pulse generator onto the transmission lines. For this purpose, it is preferable to use a solid plate in the launch region as illustrated in the ground plane sketch of Figure 8 [16]. It is noted that in the launch region, a solid plate is recommended and the mesh size can get increasingly larger as one moves away from the launch region. The mesh sizes indicated in the figure are typical values and they are governed by the particular risetimes of the electromagnetic pulse being propagated. The ground plane meshes are typically held in place by a galvanized steel framework structure which is securely attached to ground by means of concrete footings. At the perimeter of the mesh, spaced about 1 m apart, grounding rods that are about 2 m long are welded into the angle-iron framework and driven into the ground [16]. This is to provide good grounding and minimize reflections which might originate at the perimeter of the ground plane. The separation between grounding rods is chosen

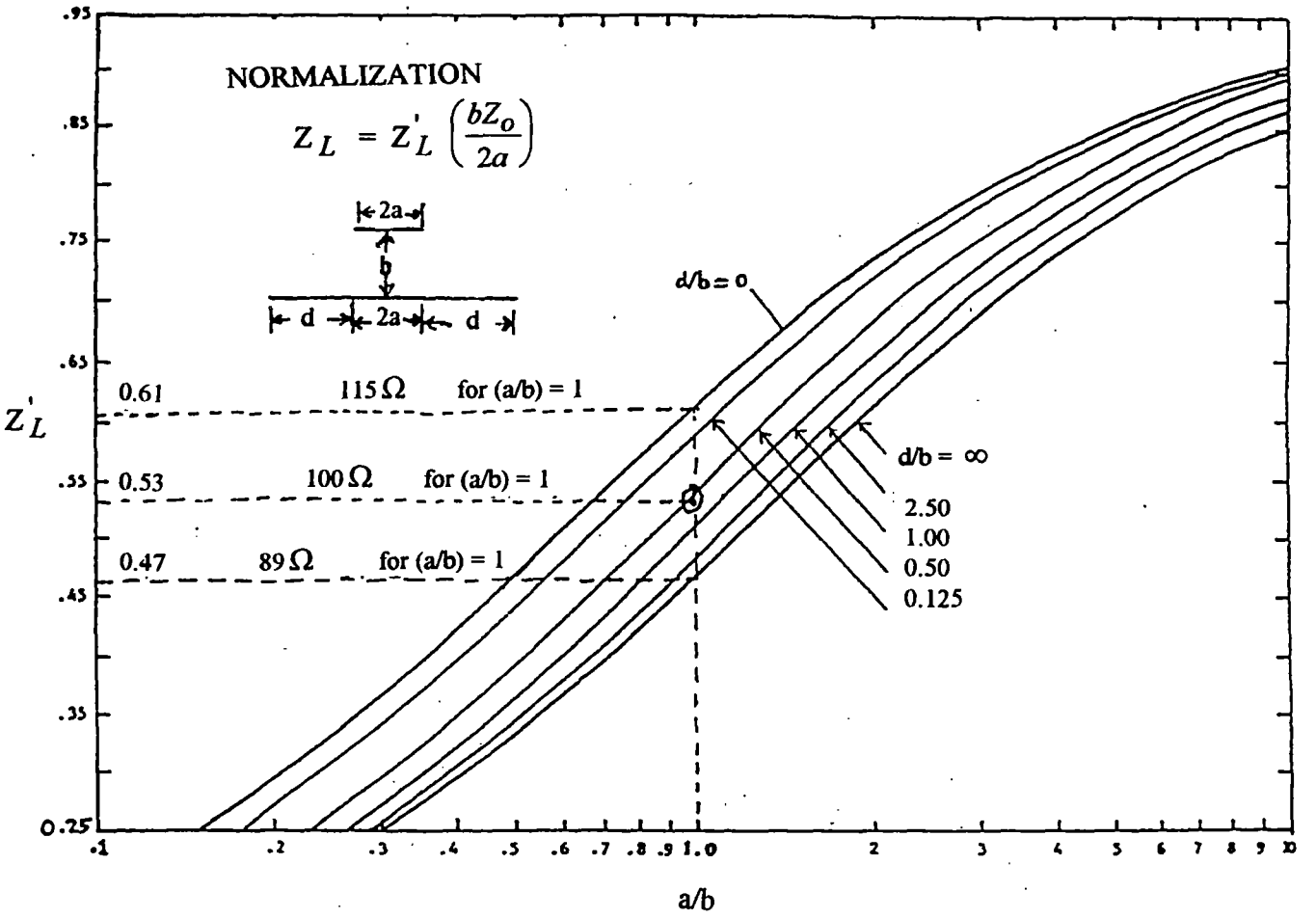

Figure 6. Normalized TEM impedance as a function of (a/b) with (d/b) as a parameter [15]

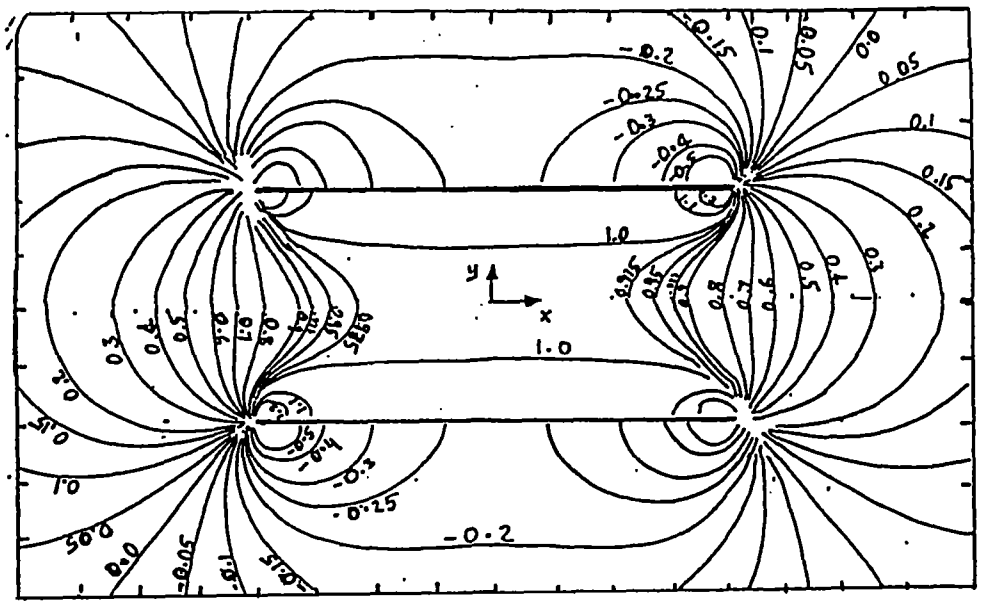

Figure 7a. Contours of constant principal electric field normalized to its value in two infinity wide plates for b/a = 0.5.

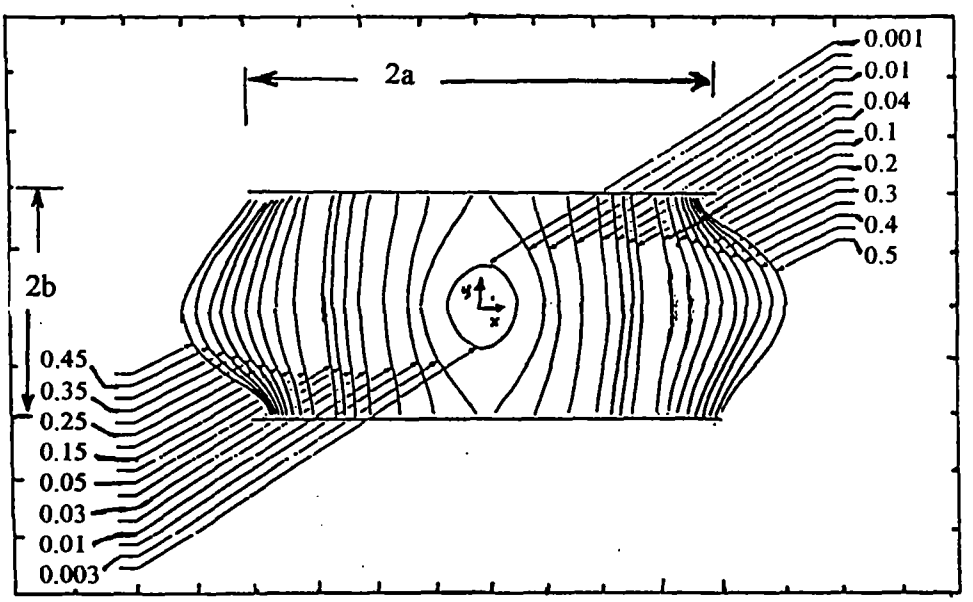

Figure 7b. Field uniformity expressed as relative deviation of the field from its value at the center for b/a = 0.5.

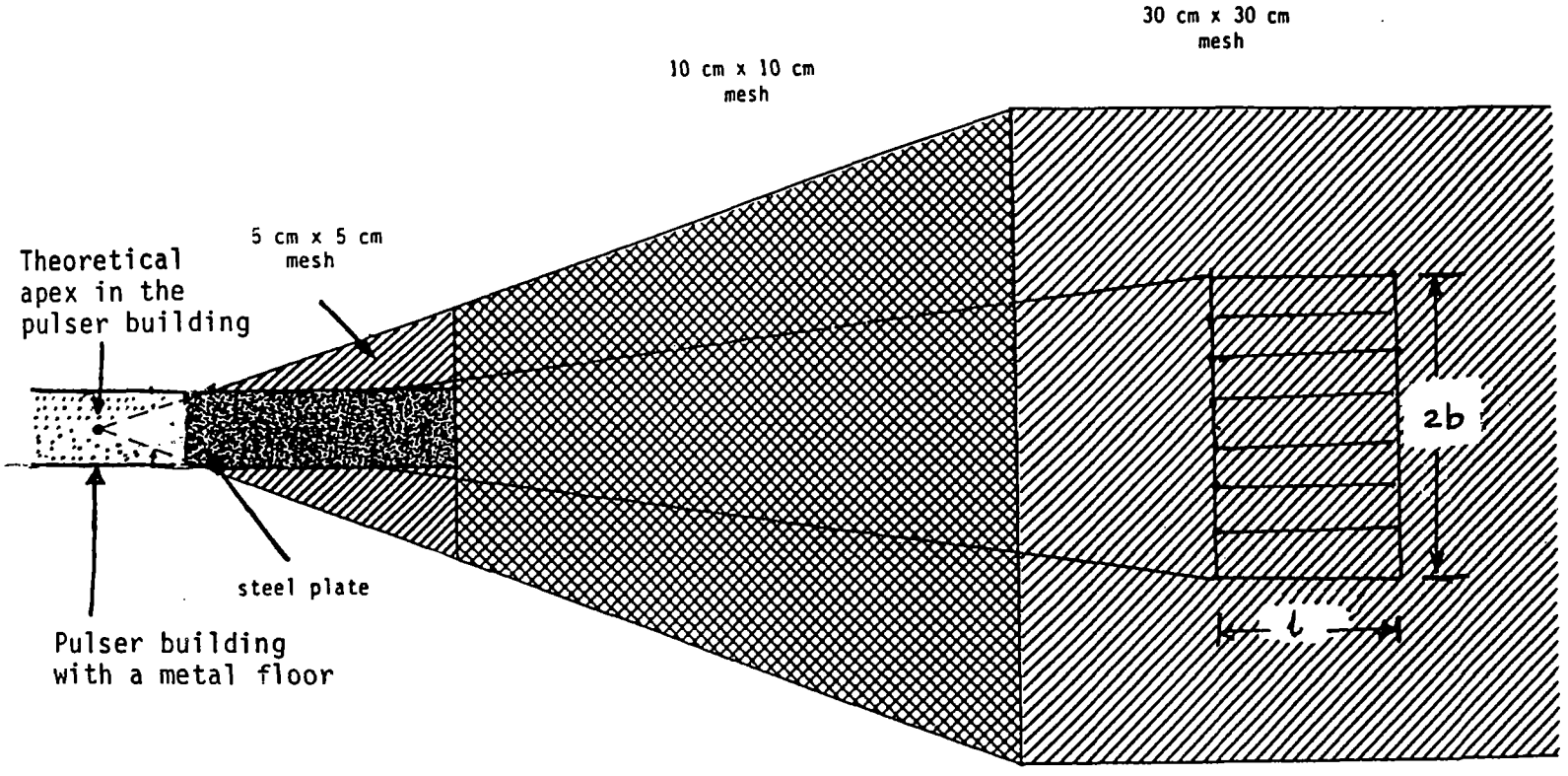

Figure 8. Ground plane layout (not to scale)

so that it corresponds to a resonant length at frequencies much higher than f_h, therefore keeping the distortion of the incident waveform small.

The dirt beneath the ground is leveled and compressed and then oiled, to stabilize it against wind and water erosion or wear from light traffic. The mesh is then stretched over the framework and welded to it. At the seams between the mesh strips, the wires are welded and stainless steel rods are driven into the ground and clamped to the mesh every meter approximately. This grounds the mesh and also keeps it from pulling up from the ground. In some facilities, asphalt has been used over the wire mesh forming the ground plane. However, the use of asphalt must be avoided in the long section of the ground plane from conical launch to the test object. A dielectric medium such as asphalt over the ground plane is a source of surface waves which is dispersive. This has also been experimentally observed [17]. It is acceptable to cover the wire mesh with asphalt, for short distances under the test object and to its side or rear for access, while bringing in heavy test objects such as a tank. A better alternative to asphalt is to use a conducting epoxy material. On the concrete pads, after the mesh is laid down, an epoxy sand mortar can be trowelled into the mesh openings, up to the thickness of the wires. This provides a level surface on which heavy vehicles and tanks can maneuver without tearing up the mesh. This solution will not degrade the electromagnetic performance of the ground plane.

A long concrete pad is also provided at the location where the termination strings connect to the ground. This pad is also edged in steel, so that the termination chains can make good electrical contact to the wire mesh of the ground plane.

4. *Transmission-Line View of Terminator*

It is evident that for the conical transmission line type of NEMP simulators, the terminator is distributed for higher-frequency performance, as distinct from a lumped element terminator for low-frequency circuits, or for transmission lines that can provide a wave receptor and basically come down to an area near the apex of the wave receptor. When the terminator is large (several meters in each direction), the desirability of a sloping "sheet-like" terminator is well established [18-20]. Sloping the termination, as illustrated in Figure 9, makes the required current distribution for an ideal termination more rapidly approach its late-time (low-frequency) value which has proved to be a useful feature in realizing good quality distributed terminations.

The previous analyses of terminations have looked at plane-wave incidence on an admittance sheet in realizing the practical terminating impedances. They are realized by series-parallel combinations of resistive elements with inductive contributions from loops of resistive strings, internal inductances and external lead inductances. In other words, such a terminator simulates an L-R sheet. One can also view the terminator (Figure 9) section as a transmission-line in itself. We observe from Figure 9 that the TEM characteristic impedance Z_c is a constant in the transmission line ($z < z_1$) and becomes a function of z in the terminating section extending from $z = z_1$ to $z = (z_1 + \ell)$. Also note that $Z_c(z) = 0$ at the end of the terminating section when $z = (z_1 + \ell)$. Let the resistive distribution in the terminating section be represented by R'(z) (Ω/m). A perfect terminator implies

$$\frac{d}{dz} Z_c(z) = - R'(z) \tag{5}$$

or

$$Z_c(z) = - \int_z^{\infty} R'(z)\, dz' \qquad \text{for } z_1 \le z \le (z_1 + \ell) \tag{6}$$

The above equation is the relationship between the characteristic impedance of the line at that cross-section in terms of the termination parameters. The termination, as seen in Figure 9 starts at $z = z_1$, and ends at $z = (z_1 + \ell)$. It comprises of two parts, the first of which are tapering metallic

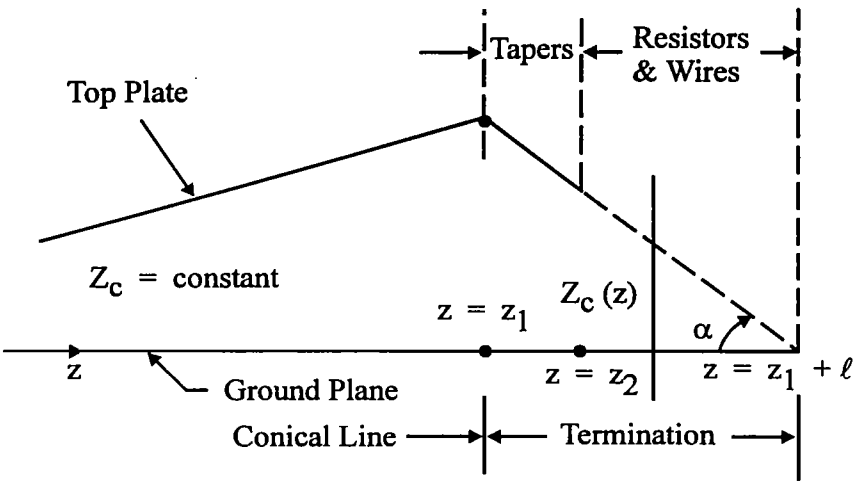

Figure 9. Side view of a distributed terminator

structures which connect to the edge of the top plate on one end and to the resistive wires at the other. This taper section extends from $z = z_1$ to $z = z_2$ and the resistive strings extend from $z = z_2$ to $z = z_1 + \ell$. In the taper section, the impedance as a function of z can be kept constant and equal to the characteristic impedance of the conical line. It is much like the conical line except it is sloping in an opposite direction to the main line. In the taper section ($z_1 \leq z \leq z_2$), the local height is decreasing as well as the local width of the top-plate. As the tapers decrease in height, they also decrease in width so as to keep $Z_c(z)$ unchanged from the value in the transmission line. When the tapers reach the wires, the impedance (thereby require height reduction) can be calculated using the formulae in [7]. For a wide top plate (a >> b), the additional height to add to the physical height for impedance calculations is

$$\Delta y = \frac{(wire\,spacing)}{2\pi} \quad \ell n \left[\frac{(wire\,spacing)}{\pi(wire\,diameter)} \right] \tag{7}$$

For a moderate to narrow top-plate width, the fields above and on the top plate change this somewhat, so that one can use Z_o ($\cong 377\,\Omega$) times a factor which can range from $\Delta y / (2a)$ to $\Delta y / a$ to estimate the impedance increase. Having chosen an α (angle of the sloping terminator), the coordinate $z = z_2$ where the taper ends is thereby determined. The tapers themselves can be triangular in shape, the base of the triangle is connected to the edge of the top-plate and the vertex of the triangle to a resistive chain. The local impedance $Z_c(z)$ for $z_1 \leq z \leq z_2$ can be approximated by that of a cylindrical transmission line, which is extensively documented in [9]. In the absence of tapers, we would have a connection (an abrupt one) between the edge of top-plate and a finite number of resistive chains which results in a scattered signal/wave back to the test object. This has also been experimentally observed in [21]. Having outlined the design principles of the taper sections, we now address in the next section the issue of matching the terminator (taper plus resistive chains) to current distribution in the top-plate, which is predominantly the TEM modal current.

5. *Matching Terminator to Current Distribution in Top-Plate*

Since the conical transmission line is designed to primarily propagate a spherical TEM wave, one can take advantage of the knowledge of the TEM current distribution in matching the terminator. If there are N resistor chains in the terminator, we require that N tapers be attached to the top-plate in such a way that there is an equal amount of current (I_t / N) out of each taper into the resistive string, where I_t is the total current flowing on the top-plate. This can be accomplished by approximating the TEM current density, $J_s(x)$ (A/m) with square root singularities (based on the conformal-transformation solution for a strip far from other objects) as follows.

$$J_s(x) \cong \frac{J_o}{\pi\sqrt{1-(x/a)^2}} \; A/m \tag{8}$$

where x is the familiar transverse coordinate and 2a is the width of the top plate. This is a fairly good approximation for the TEM current. One can also obtain a more elaborate solution including the presence of a parallel ground plane [22]. Knowing the current density distribution, we can find the width of each taper so that each taper carries equal current. The equal currents in the resistive strings avoid loop currents in the terminator and keeps the fields in the terminator region fairly uniform.

We divide the top-plate into N regions with current in each region denoted by I_n for n = 1 to N. The total current is given by

$$I_t = \sum_{n=1}^{N} I_n \quad \equiv \quad \textit{total current in the TEM mode} \tag{9}$$

and the current in any section is given by

$$I_n = \int_{x_{n-1}}^{x_n} J_s(s)\, dx \tag{10}$$

Substituting (8) into (10), we find

$$I_n = J_o \frac{a}{\pi}\left[\arcsin\left(\frac{x_n}{a}\right) - \arcsin\left(\frac{x_{n-1}}{a}\right)\right] . \qquad (11)$$

The total current is simply J_o a (Amps). Equal current in all tapers implies

$$I_n = I / N . \qquad (12)$$

If N is chosen to be an even number = 2M (e.g., N = 10, M = 5), we maintain symmetry about the center line meaning; we will have M number of tapers on each side of the center line. Now, consider m sections to the right of the center line. So the total current in these m sections is given by

$$m\left(\frac{I}{2M}\right) = \int_o^{x_m} J_s(s)\, dx \qquad (13)$$

$$m\left(\frac{J_o a}{2M}\right) = \frac{J_o a}{\pi}\left[\arcsin\left(\frac{x_m}{a}\right) - \arcsin(0)\right]$$

or

$$\frac{m}{2M} = \frac{1}{\pi}\arcsin\left(\frac{x_m}{a}\right) \qquad (14)$$

or

$$\left(\frac{x_m}{a}\right) = \sin\left(\frac{\pi m}{2M}\right) . \qquad (15)$$

An illustrative example is listed in Table 2, using the above equation for computing the base widths of the taper sections.

Table 2. Taper parameters for N = 10.	
N = 2M ; M = 5	
m	$(x_m/a) = \sin(\pi m/2M)$
1	0.309
2	0.588
3	0.809
4	0.951
5=M	1.000

The taper sections are illustrated in Figure 10 and a schematic of the terminator (taper + resistive strings) is shown in Figure 11. Some practical considerations in fabrication may include fabricating the taper sections in wire-mesh structure, fastened to a wooden support frame and, the connection points of the resistive chains to the ground plane should be such that they can be varied along a straight line and not a circular arc. The outer strings may have to be moved outward during the experimental optimization process.

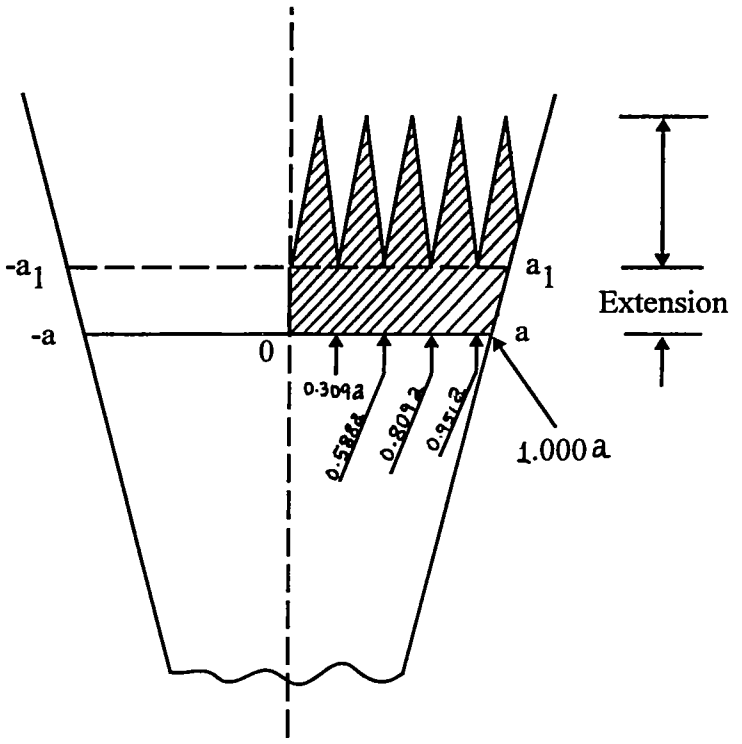

Figure 10. The taper sections at the top-plate

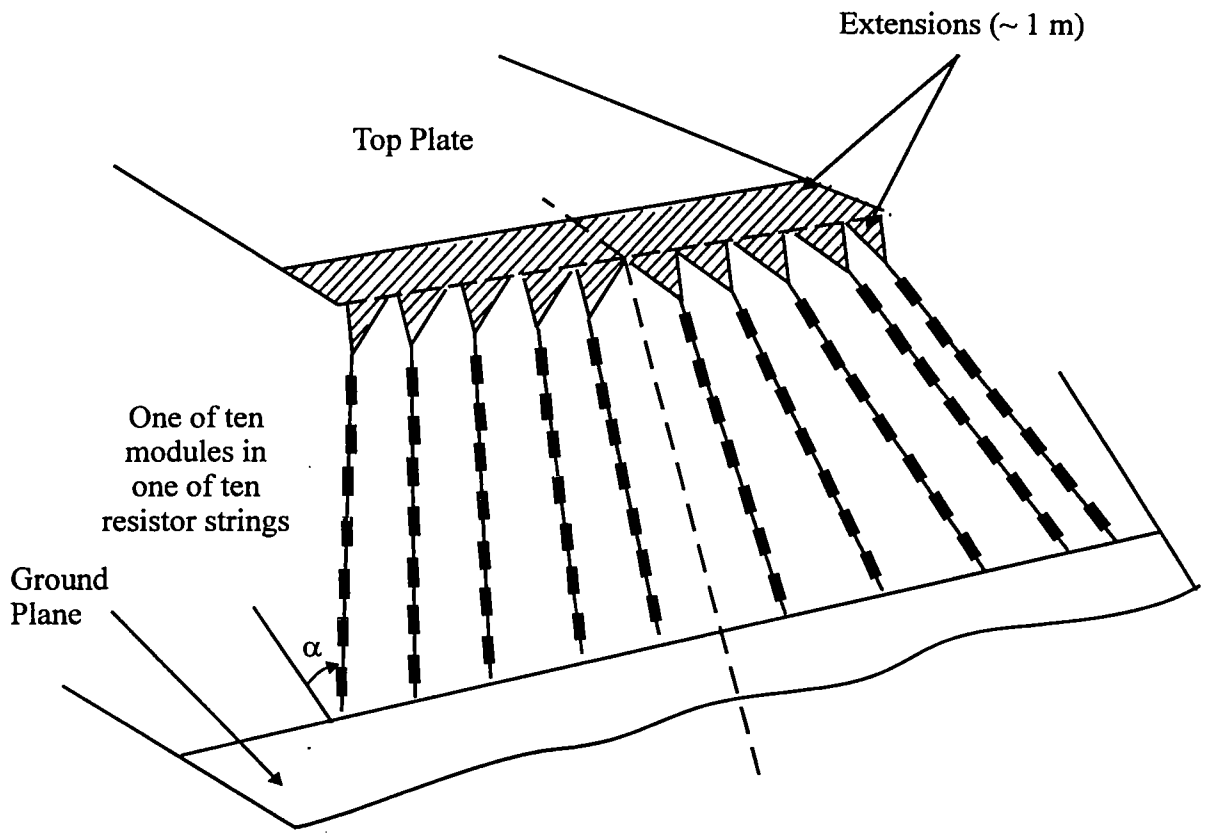

Figure 11. Schematic diagram of the terminator

6. *Optical View of Terminator*

The spectrum of frequencies contained in the electromagnetic pulse propagating in the conical transmission line typically extends from dc to hundreds of MHz. The corresponding wavelengths are ∞ to tens of cm. Since test-object heights can be up to a few meters, it is clear that the cross-sectional dimensions of the conical line can become several wavelengths at higher frequencies of the pulse spectrum. While it is true that, at these high frequencies, non-TEM modes can be supported, they cannot propagate unless they are launched. Earlier sections of this note have discussed ways of avoiding higher-TEM and non-TEM mode excitation. So, in principle, the bandwidth of the simulator is extends from dc up to an upper useful frequency f_u. This is the frequency above which the desirable modes have unacceptable amplitudes.

Having established that the TEM-like behavior extends to frequencies where the cross-sectional dimensions become several wavelengths, we now turn our attention to the terminator. At low frequencies (dc to a few MHz), the terminator which is an L-R combination works well in terminating the TEM current/wave. At high frequencies (cross-sectional dimension >> λ_s), the L-R termination is ineffective and unwanted. The requirement is that the propagating wave should simply radiate out through the terminator. Such an optical view of the terminator (ω approaching ∞) requires a sparse terminator in minimizing scattering back toward the source / test object (Figure 12a). However, one cannot completely eliminate the scattering back of the TEM wave incident on the resistive strings of the terminator, but can make the scattered wave in directions other than back toward the source/test object (Figure 12b). We view the reflections at the terminator and the ground plane as plane wave reflections, and there will be successive reflections. If r_n represent reflection coefficients, for each incidence, one has an effective reflection of

$$r_e = \prod_{n=1}^{N_r} r_n \qquad (16)$$

where r_e = effective/total reflection coefficient, r_n = are the individual coefficients ($|r_n| < 1$) and N_r being the number of reflections. N_r will be a function of the terminator slope α and the

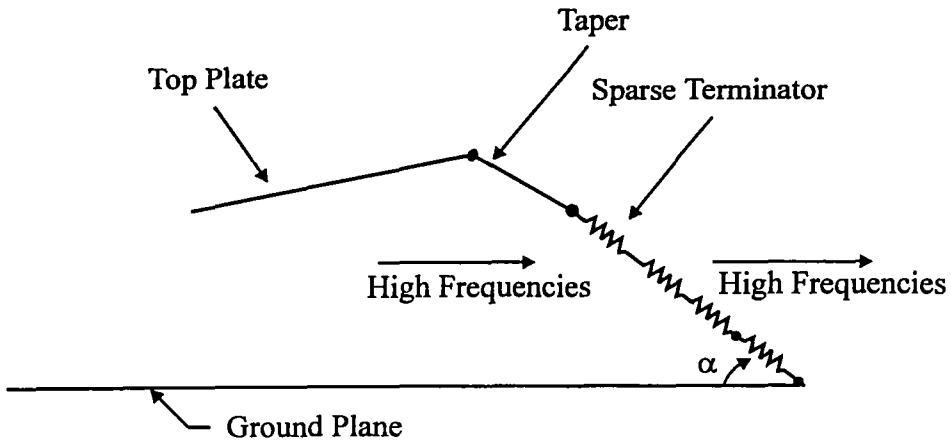

(a) Sparse terminator for radiating out the high frequencies.

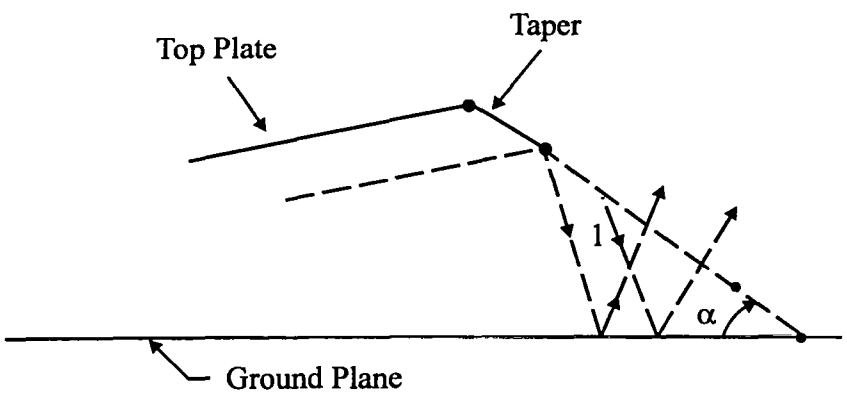

(b) Scattered ray paths at the terminator

Figure 12. Optical/high-frequency considerations of terminator.

angle of incidence. Clearly large N_r helps in reducing the scattering back toward the source/ test object.

Yet another useful technique is to stagger the resistive chains in the z or propagation direction so that any scattering back toward the working volume will not arrive at the same time or in the same phase, as illustrated in Figure 13. It is seen in Figure 13a that the resistive chains, in different planes, are parallel to each other. One might even have these planes not parallel to each other (different slope angles α_i) to further break up any coherence of the reflections at specific frequencies.

Furthermore, it is also possible to place resistive sheets along TEM-equipotential surfaces to further attenuate reflections while they propagate in directions transverse to z-coordinate. This is similar to higher-order mode suppression [23] in the input and/or output conical portions of a cylindrical-line simulator. This concept is illustrated in Figure 14. In [23] the objective of the resistive sheets was to extract energy from TE / TM modes. Compared to that, in the present situation, the resistive sheets work more efficiently in attenuating the reflections, when the reflected waves are propagating in transverse directions.

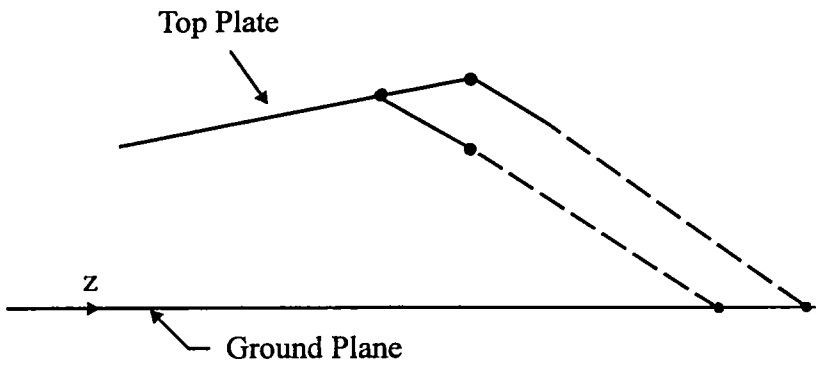

(a) Side view.

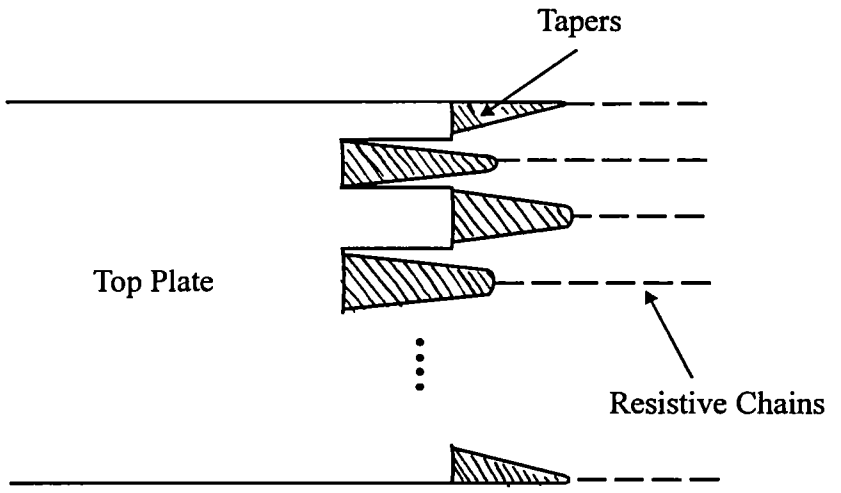

(b) Top view.

Figure 13. Staggering of the resistive chains along the direction of propagation.

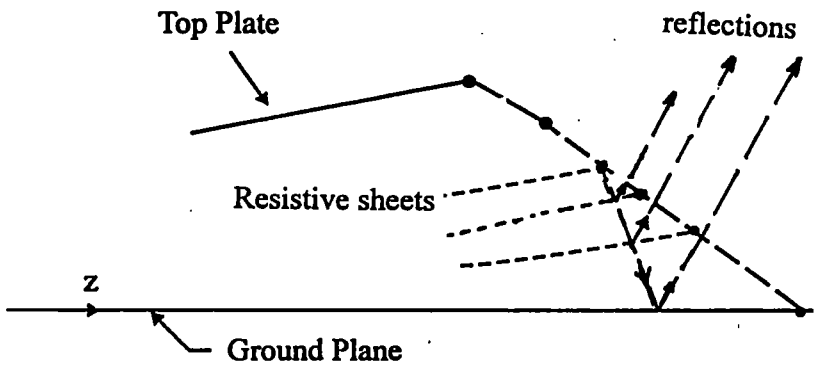

(a) Resistive sheets connected to proper potential position on resistive string.

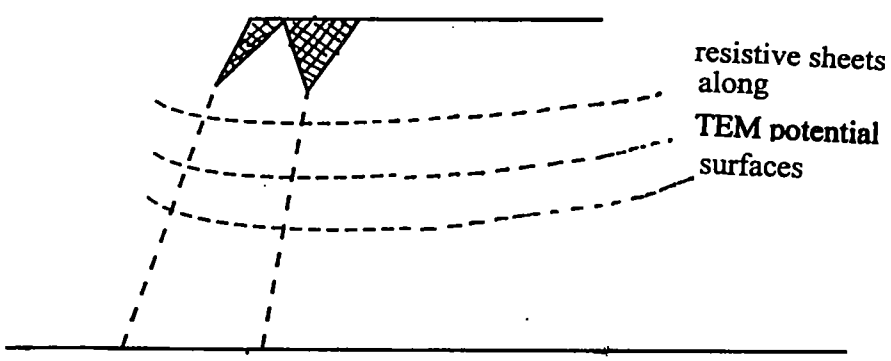

(b) Curved resistive sheets along TEM potential surfaces

Figure 14. Use of resistive sheets to attenuate reflections

7. *Equivalent Circuit of Terminator*

One can develop an equivalent circuit of the terminator in a step-by-step fashion as follows. With reference to Figure 15, let us first assume that there is no physical terminator (Figure 15a). Then at high frequencies, there is no reflection back toward the source because of outward radiation, and at low frequencies we have an open circuit. Such as open circuit termination can be modelled by a series combination of Z_c and C_t. The capacitance C_t (open circuit at low frequency) represents the fringe capacitance around the end (not the sides) of the top plate. This model is valid in the absence of a physical terminator. It is observed that at high frequencies C_t is a short circuit and the termination is Z_c which results in no reflection.

Next, we add a resistive terminator of value Z_c (Figure 15b). This then is physically present and is parallel to the previous R-C combination, resulting in a total termination Z_t of

$$Z_t = Z_c \,||\, \left(Z_c + \frac{1}{sC_t}\right) = \begin{Bmatrix} Z_c/2 \text{ as } s \rightarrow \infty \\ Z_c \text{ as } s \rightarrow 0 \end{Bmatrix} \qquad (17)$$

The above Z_t then gives a reflection coefficient of (1/3) at high frequencies and no reflection at low frequencies.

Next, we may add a series inductor L_t with the resistive termination (Figure 15c). This is not a physical inductance but it comes about anyway, because of several contributions such as: (i) intrinsic inductance of the resistors, (ii) lead inductances and (iii) external sheet/loop inductance[20, 24-29]. The TEM wave extends to ∞ from the top-plate and sides of the top-plate, represented by the external inductance. Now we have an equivalent circuit as shown in Figure 15c. Spreading out the resistor chains fills up the terminating surface and is preferable. Ideally, the currents in the terminator should match the magnetic field of the TEM mode. Practically, one can make a wide terminator, by spreading out the connections at the ground plane (Figure 15c), but it is a limited solution, since the TEM field does extend to infinity. This limitation also affects the low-frequency magnetic field at the test objects (excessive field) requiring the placement of test objects at some distance from the terminator, back toward the

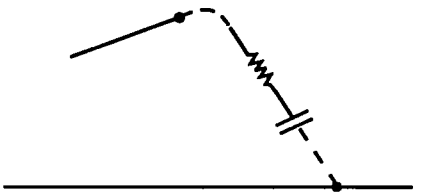

(a) Open circuit termination

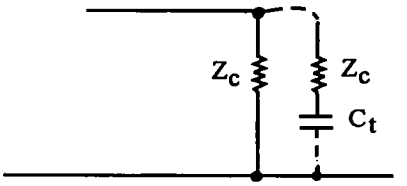

(b) Characteristic impedance (resistive) termination

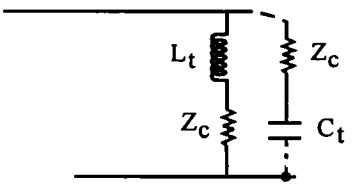

(c) Intrinsic and external inductance contributions.

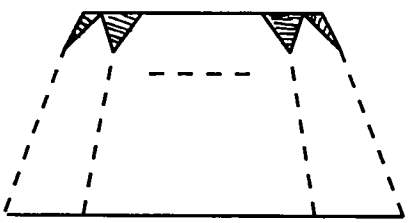

(d) Spreading of the resistive chain (reducing the inductive element)

Figure 15. Equivalent circuit development

source. In practice, the working volume should be at least one terminator height away from the terminator.

From the equivalent circuit of Figure 15c, the proper inductance value L_t is found from constraining the terminator to have

$$\begin{aligned} Z_t &= Z_c \qquad \text{for all frequencies} \\ &= (sL_t + Z_c) \,||\, \left(Z_c + \frac{1}{sC_t}\right) \\ &= \left\{ \frac{1}{(sL_t + Z_c)} + \frac{sC_t}{(1 + sC_t Z_c)} \right\}^{-1} \end{aligned} \tag{18}$$

It is seen that the above condition requires

$$\frac{L_t}{Z_c} = Z_c\, C_t \;\Rightarrow\; L_t = Z_c^2\, C_t \tag{19}$$

or the two time constants must match. If one can estimate or measure the fringe capacitance C_t, then the required inductance L_t can be computed from (18). Recall that this inductance L_t is supplied by three separate components as indicated earlier and there should be no need for a physical inductor. The need is to adjust and balance out the inductor value. It is further observed that sloping the terminator decreases the fringe capacitance C_t and thus the required inductance L_t. It is noted that the above outlined description of the required inductance from an equivalent circuit viewpoint, is approximate. More rigorous estimates of the required inductance are available and the expressions are summarized below [27,29].

$$\begin{aligned} L_{i,a} &\equiv \text{ internal array inductance } = L_i \text{ x } (N_s / N_p) \\ L_{e,a} &\equiv \text{ external array inductance } = \left(\frac{\ell_R}{w_T}\right) N_s \; L_{s,e} \\ L_{e,f} &\equiv \text{ external inductance associated with the fringe fields} \end{aligned} \tag{20}$$

The total available inductance, without adding any physical inductor is the sum of the three inductive components listed in (20). Various quantities appearing in (20) are:

$$L_{s,e} \equiv \left(\frac{\mu_o}{2\pi}\right) d \sin^2(\alpha) \ell n\left(\frac{d_s}{2\pi r_w}\right) \tag{21}$$

$L_i \equiv$ intrinsic inductance of an individual resistor, $N_s \equiv$ number of series resistors in each string

$N_p \equiv$ number of parallel resistor strings, $w_T \equiv$ width of the terminator ($\geq 2b$),

$\ell_R \equiv$ length of individual resistor (including interconnecting leads),

$d_s \equiv$ average separation between resistor strings,

$r_w \equiv$ resistor radius (average, including interconnecting leads),

$\alpha \equiv$ slope angle of the distributed terminator (average with respect to top plate and ground plane)

Furthermore, the required inductance L_R for a good match at high frequencies, is given by [20,24],

$$L_R = \left(\frac{\ell_R}{w_T}\right) h_T \mu_o \sin(\alpha) \beta_h^{(opt)} f_a \tag{22}$$

where $\beta_h^{(opt)} \cong \sin(\alpha)$ is estimated from the data in [20] and f_a is a factor with a value between 0 and 1 to account for the fringe fields. From the above listed expressions it is possible to estimate the required inductance in the distributed terminator and provide for it in the terminator design.

While L_t is not a physical inductor, it is influenced by the terminator slope angle α, the intrinsic inductances of resistors, the lead inductances, and the external sheet inductance. The control of L_t is obtained by several factors such as choosing α and N, spreading of resistor chains and varying the diameter of the interconnecting leads between resistors. Careful monitoring of the reflected signal in the working volume and near the terminator can lead to an optimal distributed terminator for this class of NEMP simulators [21,28].

8. *Tuning the Terminator*

In foregoing sections, we have discussed several design principles in the fabrication of a distributed terminator. The formulas indicated are only approximate, but adequate to design the initial parameters of the terminator for experimental optimization. Two techniques that are available for optimizing the terminator performance are:

(1) measure the electric or magnetic field in the working volume and look for the reflected signal that will appear on the decay portion of the waveform after a time corresponding to twice the travel time from the observation location and the terminator [21,29];

(2) measure simultaneously the electric and the magnetic field; a linear combination of the two can cancel out the incident field and produce a measurement of only the reflected field [29,30].

Both of the above techniques have been successfully used in past efforts in the experimental optimization of distributed terminator parameters. The two constraints that are useful in the optimization process are:

Constraint 1: The reflection into TEM mode going back toward the source should be minimized in a broadband sense. This is accomplished by measuring TDR (in time domain) and VSWR (broadband of frequencies) at input terminals to the simulator noting that the higher-order modes are evanescent near the source.

Constraint 2: Without violating constraint 1 above, amplitudes of higher-order modes (TE and TM) in the working volume have to be minimized. This is accomplished by a simultaneous measurement of electric and magnetic fields, and considering a linear combination that cancels out the incident field. Assuming a small reflected TEM wave (constraint 1), the remaining signal is contributed by higher-order modes. One can also detect the presence of higher-order modes (TE and TM) by measuring the radial components of electric and magnetic fields which are absent in the TEM wave.

9. *Summary*

Conical transmission-line type of NEMP simulators have proved to be efficient and practical structures for EMP testing of various sized objects (electronic subsystems to tanks). Both transient pulse generators and low-level CW excitations are possible and generally they simulate a vertically polarized, horizontally propagating electromagnetic wave. It is basically a long transmission line that is terminated in a physically large and distributed terminator. The transmission line itself is identical to the wavelauncher in the older design of cylindrical transmission line. The distributed terminator then becomes the key component of the conical line. Various design principles of conical transmission lines such as avoiding the non-TEM modes, top-plate and ground plane considerations and the terminator design in detail are outlined in this note. Such simulators have been employed with pulse risetimes of the order of 5 nsec, with the upper 3 dB roll of frequency f_u of 70 MHz. As the pulse risetime decreases to 1 nsec for example, the upper frequency f_u increases to 350 MHz. Additional considerations concerning the pulser (such as electromagnetic lenses), and more stringent requirements on the ground plane and top plate will become necessary to propagate a pulse with 1 nsec risetime.

References

[1] C.E.Baum, "EMP Simulators for Various Types of Nuclear EMP Environments: An Interim Categorization," Sensor and Simulation Note 240, January 1978 and Joint Special Issue on the Nuclear Electromagnetic Pulse, IEEE Trans. Antennas and Propagation, January 1978, pp. 35-53, and IEEE Trans. EMC, February 1978, pp. 35-53.

[2] D.V.Giri, T.K.Liu, F.M.Tesche, and R.W.P.King, "Parallel Plate Transmission Line Type of EMP Simulators: A Systematic Review and Recommendations," Sensor and Simulation Note 261, April 1980.

[3] J.C.Giles, "A Survey of Simulators of EMP Outside the Source Region, Some Characteristics and Limitations," presented at NEM 84, Baltimore, Maryland, July 1984.

[4] F.C.Yang and K.S.H.Lee, "Impedance of A Two-Conical-Plate Transmission Line," Sensor and Simulation Note 221, November 1976.

[5] F.C.Yang and L.Marin, "Field Distributions on a Two-Conical Plate and a Curved Cylindrical Plate Transmission Line," Sensor and Simulation Note 229, September 1977.

[6] T.L.Brown, D.V.Giri, and H.Schilling, "Electromagnetic Field Computation for a Conical Plate Transmission Line Type of Simulator," DIESES Memo 1, 23 November 1983.

[7] C.E.Baum, "Impedances and Field Distributions for Parallel-Plate Transmission Line Simulators," Sensor and Simulation Note 21, 6 June 1966.

[8] T.L.Brown and K.D.Granzow, "A parameter Study of Two-Parallel-Plate Transmission Line Simulators of EMP Sensor and Simulation Note 21," Sensor and Simulation Note 52, 19 April 1968.

[9] C.E.Baum, D.V.Giri, and R.D.Gonzalez, "Electromagnetic Field Distribution of the TEM Mode in a Symmetrical Two-Parallel-Plate Transmission Line," Sensor and Simulation Note 219, 1 April 1976.

[10] C.E.Baum, T.K.Liu, and F.M.Tesche, "On the Analysis of General Multiconductor Transmission Line Networks," Interaction Note 350, November 1978, and contained in C.E.Baum, "Electromagnetic Topology for the Analysis and Design of Complex Electromagnetic Systems," pp.467-547, in J.E. Thompson and L.H.Luessen (eds.), *Fast Electrical and Optical Measurements*, Martinus and Nijhof, Dordecht, 1986.

[11] C.E.Baum, "Removing Differential Resonances from Array," SIEGE memo 14, 11 June 1970.

[12] D.A.Hill and J.R.Wait, "Theoretical and Numerical Studies of Wire Mesh Structures," Sensor and Simulation Note 231, 10 June 1977.

[13] C.D.Taylor and G.A.Steigerwald, "One the Pulse Excitation of A Cylinder in A Parallel Plate Waveguide," Sensor and Simulation Note 99, March 1970.

[14] R.W.Latham and K.S.H.Lee, "Electromagnetic Interaction Between a Cylindrical post and a Two-Parallel-Plate Simulator," Sensor and Simulation Note 111, 1 July 1970.

[15] G.W.Carlisle, "Impedance and Fields of Two Parallel Plates of Unequal Breadths," Sensor and Simulation Note 90, 1969.

[16] C. Zuffada and D.V.Giri, "Ground Plane Design Considerations," INSIEME Memo 4, 2 February 1991.

[17] J.C.Giles (Private Communication concerning measurements in SIEM II).

[18] C.E.Baum, "Admittance Sheets for Terminating High-Frequency Transmission Lines," Sensor and Simulation Note 53, 18 April 1968.

[19] R.W.Latham and K.S.H.Lee, "Termination of Two Parallel Semi-infinite Plates by A Matched Admittance Sheet," Sensor and Simulation Note 68, January 1969.

[20] C.E.Baum, "A Sloped Admittance Sheet Plus Co-planar Conducting Flanges As A Matched Termination of A Two-Dimensional Parallel-Plate Transmission Line," Sensor and Simulation Note 95, December 1969.

[21] S.Garmland, "Electromagnetic Characteristics of the Conical Transmission Line EMP Simulator SAPIENS," SAPIENS Memo 11, February 1986.

[22] R.W.Latham, K.S.H.Lee and G.W.Carlisle, "Division of a Two-Plate Line into Sections with Equal Impedance," Sensor and Simulation Note 85, July 1969,

[23] D.V.Giri, C.E.Baum, and H.Schilling, "Electromagnetic Considerations of A Spatial Modal Filter for Suppression of Non-TEM Modes in the Transmission Line Type of EMP Simulators," Sensor and Simulation Note 247, 29 December 1978.

[24] D.L.Wright, "Sloped Parallel Resistive Rod Terminations for Tw0-Dimesional Parallel-Plate Transmission Lines," Sensor and Simulation Note 103, 7 May 1970.

[25] A.D.Varvatsis and M.I.Sancer, "Performance of an Admittance Sheet Plus Coplanar Flanges as a Matched Termination of a Two-Dimensional Parallel-Plate Transmission Line, I. Perpendicular Case" Sensor and Simulation Note 163, January 1973.

[26] A.D.Varvatsis and M.I.Sancer, ""Performance of an Admittance Sheet Plus Coplanar Flanges as a Matched Termination of a Two-Dimensional Parallel-Plate Transmission Line, II. Sloped Admittance Sheet," Sensor and Simulation Note 200, June 1974.

[27] C.E.Baum, "Resistances and Inductances for Some Specific Terminator Sizes for ATLAS I and II," 21 December 1973.

[28] D.V.Giri, "Terminator Design for SAPIENS-II," SAPIENS Memo 12, December 1990.

[29] D.V.Giri, C.E.Baum, C.M.Wiggins, W.D.Collier, and R.L.Hutchins, "An Experimental Evaluation and Improvement of the ALECS Terminator," ALECS Memo 8, May 1977.

[30] E.G.Farr and J.S.Hofstra , "An Incident Field Sensor for EMP Measurements," Sensor and Simulation Note 319, November 1989, and IEEE Trans. EMC, 1991, pp.105-112.